

Stem Cell Reports, Volume 16

Supplemental Information

**A Scalable Suspension Platform for Generating High-Density Cultures
of Universal Red Blood Cells from Human Induced Pluripotent Stem
Cells**

**Jaichandran Sivalingam, Yu SuE, Zhong Ri Lim, Alan T.L. Lam, Alison P. Lee, Hsueh Lee
Lim, Hong Yu Chen, Hong Kee Tan, Tushar Warriar, Jing Wen Hang, Nazmi B. Nazir, Andy
H.M. Tan, Laurent Renia, Yui Han Loh, Shaul Reuveny, Benoit Malleret, and Steve K.W.
Oh**

Supplementary Information

A scalable suspension platform for generation of high density cultures of universal red blood cells from human induced pluripotent stem cells

Jaichandran Sivalingam, Yu SuE, Lim Zhong Ri, Alan Tin Lun Lam, Alison P.Lee, Hsueh Lee Lim, Hong Yu Chen, Hong Kee Tan, Tushar Warriar, Jing Wen Hang, Nazmi B.Nazir, Andy Hee Meng Tan, Laurent Renia, Yui Han Loh, Shaul Reuveny, Benoit Malleret and Steve Kah Weng Oh.

Inventory of Supplemental Information

Supplemental Table and Figures

Table S1: List of genes identified based on publication for comparison of erythroid cells differentiated from hiPSC and adult CD34 cells.

Table S2. List of primers used in this study.

Figure S1: Overview of agitation suspension culture differentiation platform.

Figure S2: Characterization of hiPSC erythroid cells differentiated in shake-flasks.

Figure S3: Characterization of hiPSC erythroid cells differentiated in shake-flasks.

Figure S4: Spinner culture differentiation of fibroblast derived hiPSC FR202.

Figure S5: Transcriptome analysis of HiPSC vs Adult differentiated erythroid cells.

Figure S6: Terminal maturation and functional characterization of hiPSC and adult CD34 differentiated RBCs.

Figure S7: Terminal maturation and functional characterization of hiPSC and adult CD34 differentiated RBCs.

Supplemental Experimental Procedures

Figure S1 Development of agitation suspension culture differentiation protocol

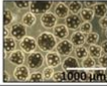
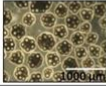
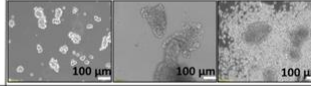





		Stage	iPSC expansion	Mesoderm induction	Hematopoietic induction	Erythroblast expansion	Erythroblast maturation
		Duration	7 days	3 days	14 days	14 days	14-21 days
		Medium	mTeSR1	Stemline II Day 0: BMP4, VEGF, Activin A, CHIR Day 1: BMP4, VEGF, Activin A Day 2: BMP4, VEGF, Activin A, bFGF, β -Estradiol, SCF	Stemline II Day 3: BMP4, VEGF, bFGF, β -Estradiol, SCF, IGF2, TPO, Heparin, IBMX Day 7: BMP4, VEGF, bFGF, β -Estradiol, SCF, IGF2, TPO, Heparin, IBMX, SR1 Day 11: BMP4, SCF, Flt3-L, IL3, EPO, IBMX	Stemline II SCF, EPO, IL3, hydrocortisone, holo-transferrin, Erycte, Serum Replacement 3, Pluripotin	IMDM EPO, 10% human plasma, holo-transferrin, insulin, mifipristone
		Culture condition	Agitation	Agitation	Agitation	Agitation	Agitation
							
Scalable culture platform							
6 well ULA plates		Seeding density: Fold-expansion: Total volume: Expanded cell numbers:	2 x 10 ⁵ cells/ml 10-14 5 ml 1-1.4 x 10 ⁷	1 x 10 ⁶ cells/ml 1-3 5 ml 2.5-7.5 x 10 ⁷	1.25 -1.75 x 10 ⁵ cells/ml 10-30 5 ml 0.625 - 2.67 x 10 ⁷	2.5 x 10 ⁵ cells/ml 100 5 ml 1.25 x 10 ⁸	1 x 10 ⁶ cells/ml N.A 5 ml 5 x 10 ⁶
		Seeding density : Fold-expansion : Total volume: Expanded cell numbers:	2 x 10 ⁵ cells/ml 10-14 5 ml 1-1.4 x 10 ⁷	1 x 10 ⁶ cells/ml 1-3 5 ml 5 x 10 ⁶	Seeding density: 1.25 -1.75 x 10 ⁵ cells/ml Fold-expansion: 10-30 Total volume: 10 ml Expanded cell numbers: 1.25 - 5.25 x 10 ⁷	2.5 x 10 ⁵ cells/ml 100 10 ml 2.5 x 10 ⁸	1 x 10 ⁶ cells/ml N.A 10 ml 1 x 10 ⁷
125 ml spinner flasks		Seeding density: Fold-expansion: Total volume: Expanded cell numbers:	2 x 10 ⁵ cells/ml 10 50 ml 1.25 x 10 ⁸	1.2 x 10 ⁶ cells/ml 1-1.4 50 ml 8.2 x 10 ⁷	2.5 x 10 ⁵ cells/ml 10-30 50 ml 1.25 - 3.75 x 10 ⁸	2.5 x 10 ⁵ cells/ml 100 100 ml 1 x 10 ⁹	1 x 10 ⁶ cells/ml N.A 100 ml 1 x 10 ⁸

Figure S1: Overview of agitation suspension culture differentiation platform. Schematic of suspension culture continuous agitation differentiation process comprising of hiPSC expansion, mesoderm induction, hematopoietic induction, erythroblast expansion and erythroblast maturation. Representative bright-field images of microcarrier-cell aggregates and/or differentiating cells are shown. The differentiation process was progressively scaled-up from 6 well ULA plates to 50 shaker flasks to 125 ml spinner flasks. The initial seeding density, fold-expansion, total volume and total cells derived after expansion are reported for each stage of differentiation.

Figure S2 Hematopoietic differentiation from hemogenic endothelial clusters in suspension differentiation protocol

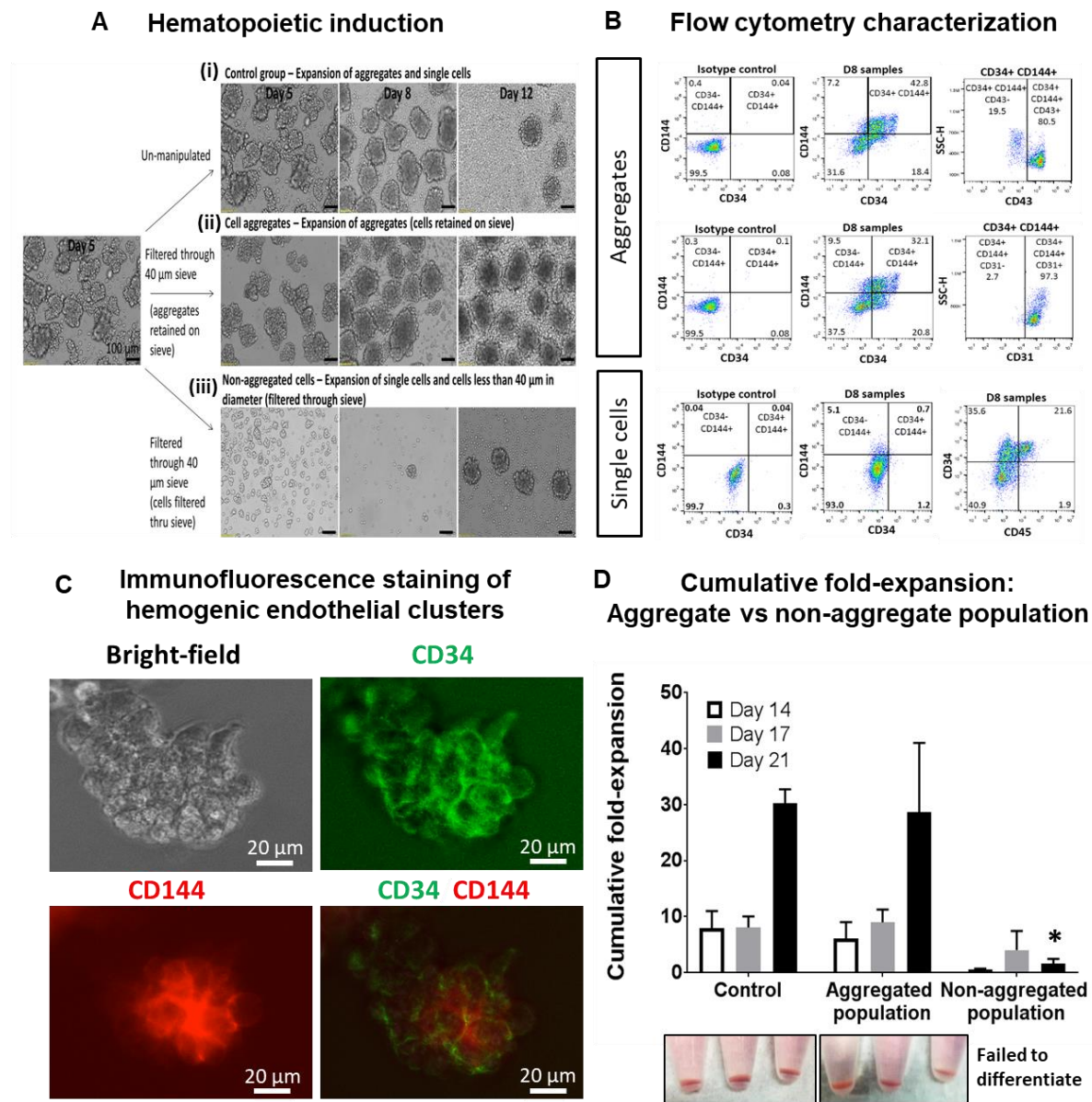
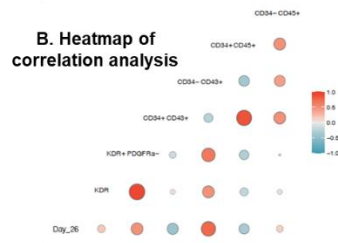
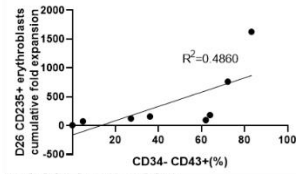


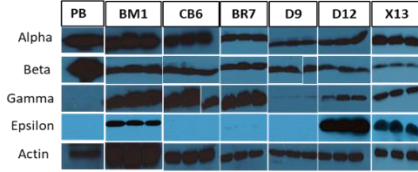
Figure S2: Characterization of hiPSC erythroid cells differentiated in shake-flasks. (A) At day 5 of differentiation, small aggregates and single cells are observed. Differentiation was performed on 3 experimental groups as follows: (i) Un-manipulated control group consisting of aggregates and single cells; (ii) cell aggregates retained following straining through 40 μ m cell-strainers; (iii) single cells derived following straining through 40 μ m cell-strainers. Representative bright-field images of differentiating cells from day 5 - day 12 are shown. (B) Cells from un-manipulated control group on day 8 of differentiation were separated by straining into aggregate and single cell population and characterized by FACS for identification of hemogenic endothelial population (CD34+CD144+CD31+/CD43+) and pan-hematopoietic progenitors (CD34+CD45+). (C) Immunofluorescence staining of day 8 cell aggregates identifies hemogenic endothelial clusters with co-expression of CD34 (green) and CD144 (red) markers. (D) Cumulative fold-expansion of differentiated cells following 21 days of differentiation of cells from groups I (control), II (aggregated population) and III (non-aggregated population). Data represent mean \pm SD with at least 3 independent replicates. Corresponding hemoglobinized cell pellets are shown below graph. Note that single cells from non-aggregated population failed to differentiate further.

Figure S3 Characterization of hiPSC erythroid cells differentiated in shake-flasks

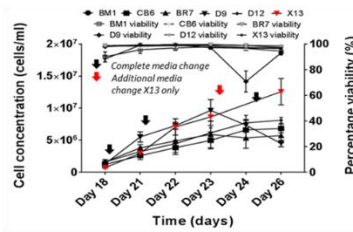
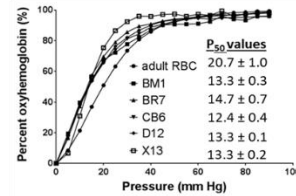
A. Correlation analysis between the D26 erythroblasts yield and CD34- CD43+ marker of 8 hiPSC cell lines



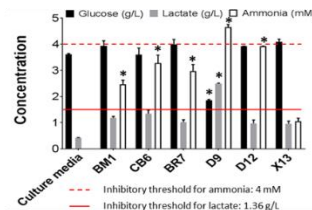
C. Hemoglobin Immunoblot



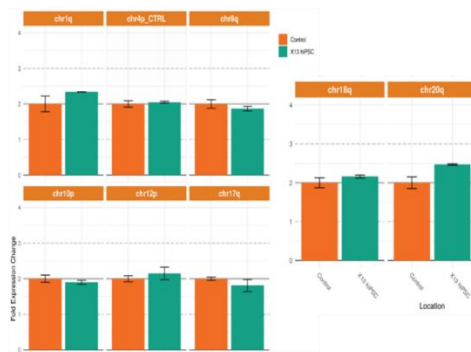
D. Oxygen equilibration



F. Metabolite measurements



G. Pluripotent stem cell Genetic Analysis



H. iCS-digital™ Pluri test



Figure S3: Characterization of hiPSC erythroid cells differentiated in shake-flasks. (A) Correlation analysis between the D26 erythroblasts yield and CD34- CD43+ marker of 8 hiPSC cell lines. (B) Heatmap of correlation analysis between the D26 erythroblasts yield and different hematopoietic markers. (C) Cell lysates from peripheral blood (PB) and erythroblasts differentiated from BM1, CB6, BR7, D9 and D12 (day 26 post differentiation) were immunoblotted with alpha, beta, gamma, epsilon human hemoglobin subtypes. *Insufficient samples for IMR90 and FR202. (D) Oxygen equilibrium curves of adult RBCs (●), hiPSC differentiated erythroblasts BM1 (■), BR7 (▲), CB6 (▼), D12 (◆) and X13 (□). Corresponding p₅₀ values are presented. *Insufficient samples for IMR90, FR202 and D9. (E) Cell concentration (cells/ml) and % viability during erythroblast expansion. Black arrows indicate complete media change for all cultures while red arrow indicates additional complete media change for X13 only. (F) Measurements of glucose (g/L), lactate (g/L) and ammonia (mM) from culture supernatants of different hiPSC erythroid cells and fresh culture media on day 24 of differentiation. Red solid and dotted lines indicate inhibitory threshold for lactate (1.36 g/L) and ammonia (4 mM) respectively. *p<0.05 for comparison against X13. (G) Recurrent karyotypic abnormalities in hiPSCs were evaluated by a qPCR-based method using hiPSC genetic analysis kit. Graphical representation of copy numbers for each locus for normal control genomic DNA and X13 hiPSC line are shown. (H) Genomic DNA extracted from X13 hiPSC derived erythroblasts (Day 24 of differentiation) were subjected to iCS-digital™ pluri test to evaluate for common genomic abnormalities. (Top) Copy number values of 24 genomic regions evaluated and colour coded accordingly (Loss (orange): 1 to 1.4 copies; Normal (green): 1.6 to 2.4; Gain (purple): 2.6 to 3) show normal copies for X13 erythroblast. (Bottom): Graphical representation of copy number values for each of the 24 chromosomal regions evaluated for X13 erythroblasts. Statistical tests were performed on the pooled data from at least 3 independent replicates.

Figure S4 Scale-up of hiPSC differentiation in 125 ml and 500 ml spinner flasks

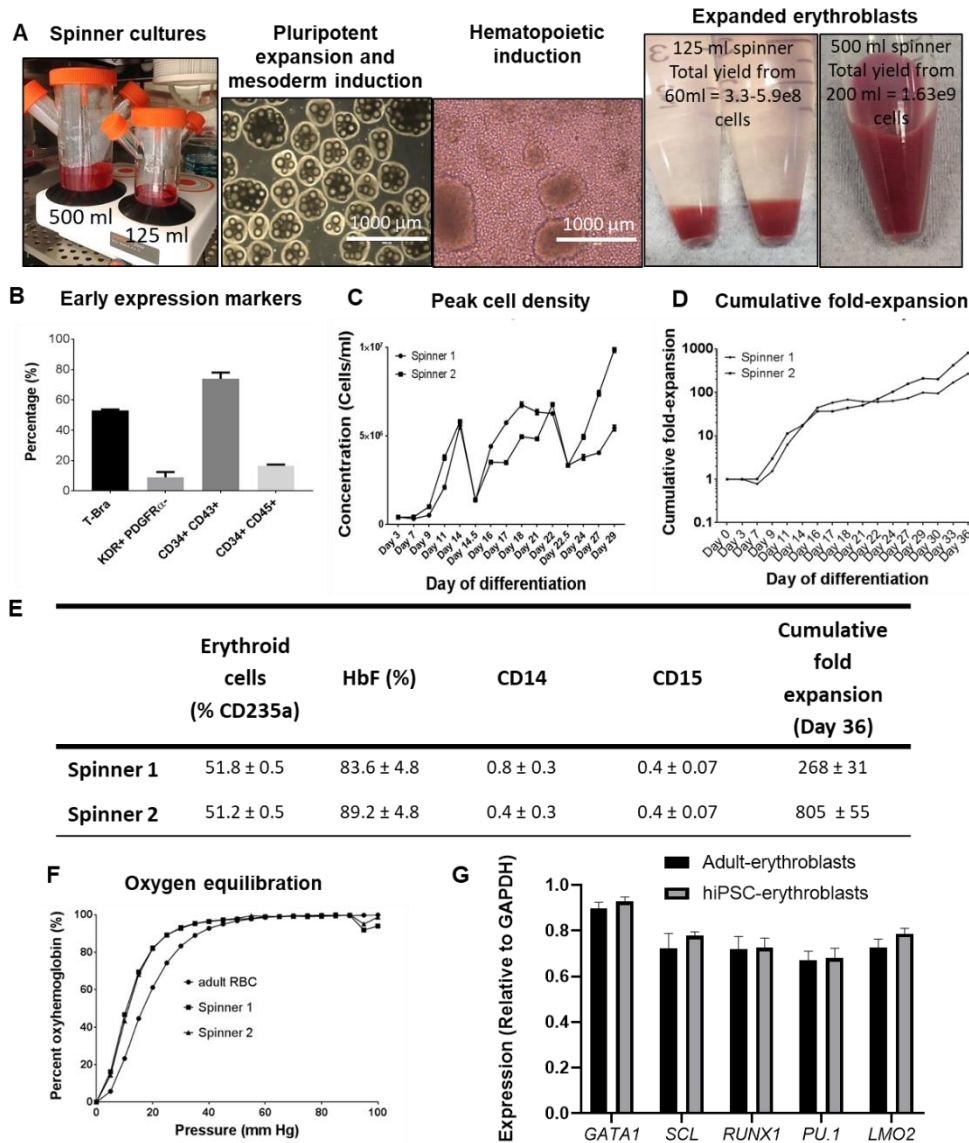


Figure S4: Spinner culture differentiation of fibroblast derived hiPSC FR202. (A) Image showing hiPSC erythroid cells cultured in 125ml and 500ml spinner culture flasks, MC-hiPSC cell aggregates during pluripotent expansion and mesoderm of differentiation, single cells and aggregates during hematopoietic induction and hemoglobinized erythroblast cell pellets from 125ml and 500ml spinner flasks (total number of cells indicated in image) respectively at the end of culture period (Day 30-36). (B) FACS percentage of cells expressing primitive streak/early mesoderm marker (T-bra), hematopoietic mesoderm marker (KDR+PDGFR α -) and hematopoietic progenitor markers (CD34+CD43+ and CD34+CD45+). (C) Cell concentration and (D) cumulative fold-expansion during the differentiation process in spinner culture flasks. Arrows indicate time-points when cells were reseeded at low density. (E) Table showing FACS summary of CD235a+ erythroid cells, fetal hemoglobin (HbF), myelomonocytic populations (CD14/CD15) and cumulative fold expansion on day 36 of differentiation. (F) Oxygen equilibrium curves of adult RBCs (●) and FR202 differentiated erythroblasts (Day 36 post differentiation) from spinner flasks 1 (■) and 2 (▲). Corresponding p50 values are presented. (G) Comparison between erythroid cells differentiated from adult CD34+ and from hiPSCs based on microarray data. There is no significant difference in the erythropoiesis induction related gene expression levels (in Fig. 3F) between the adult and hiPSC derived erythroblasts. The graph above represents these values after normalization to a control gene (*GAPDH*). Statistical tests were performed on the pooled data from at least 3 independent replicates.

Figure S5 Transcriptome analysis of HiPSC vs Adult differentiated erythroid cells

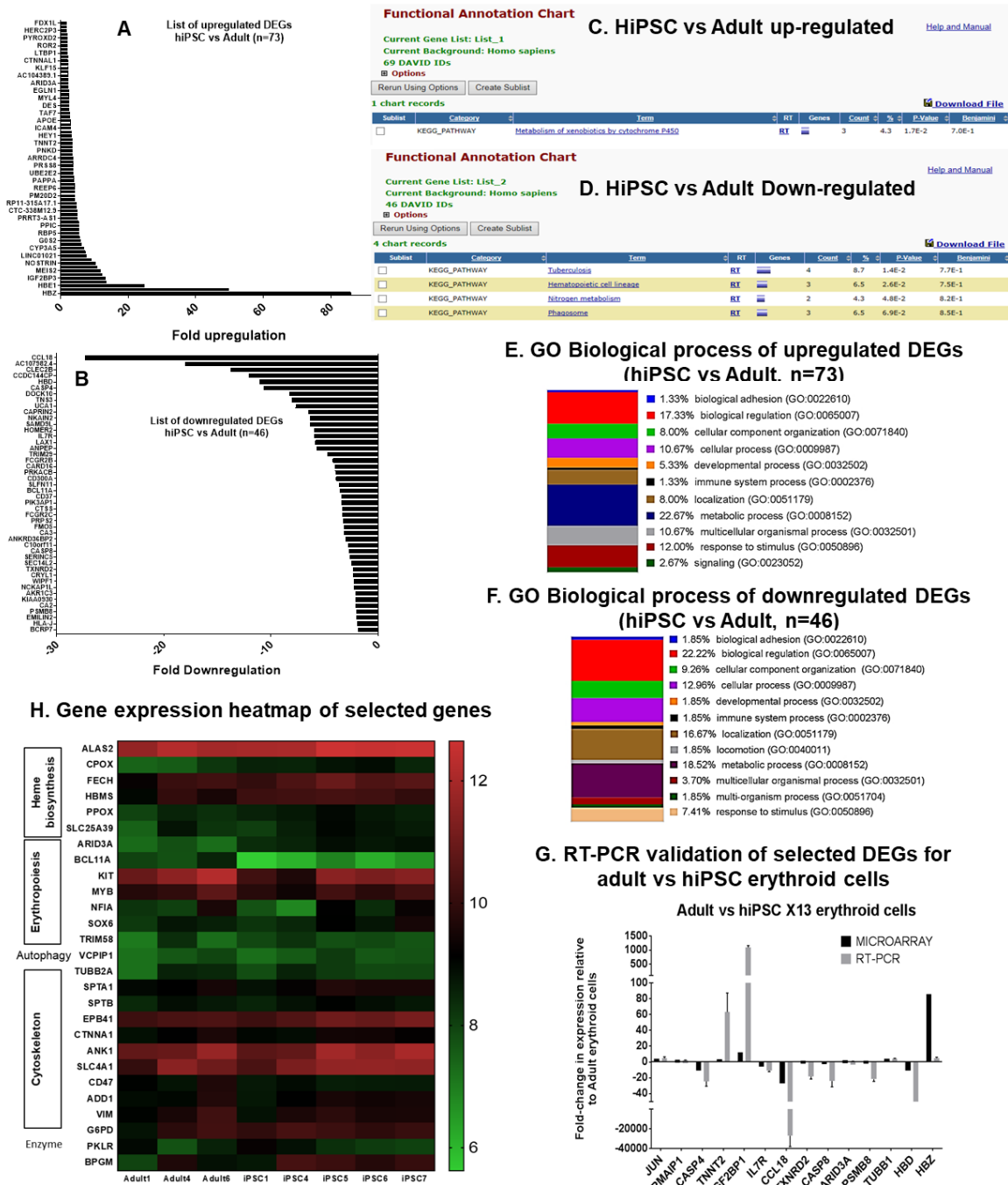


Figure S5: Transcriptome analysis of HiPSC vs Adult differentiated erythroid cells. Fold-change in expression of (A) up-regulated and (B) down-regulated DEG for comparison of erythroid cells from hiPSC vs Adult (X13 donor). Mapping of hiPSC vs adult (C) upregulated DEGs and (D) downregulated DEGs using DAVID Functional annotation analysis. Bar chart showing gene ontology of biological processes of (E) upregulated and (F) downregulated DEGs for comparison of erythroid cells from hiPSC vs Adult. (G) Comparison of fold-change in DEGs of hiPSC differentiated erythroid cells relative to adult differentiated erythroid cells validated by RT-PCR in comparison with microarray outcomes. (H) Heatmap (normalized expression signal intensity) of selected genes based on publications categorized according to molecular functions (heme biosynthesis, erythropoiesis, autophagy, cytoskeleton, enzyme) for comparison between adult and hiPSC samples.

Figure S6 Terminal maturation and functional characterization of hiPSC erythroblast

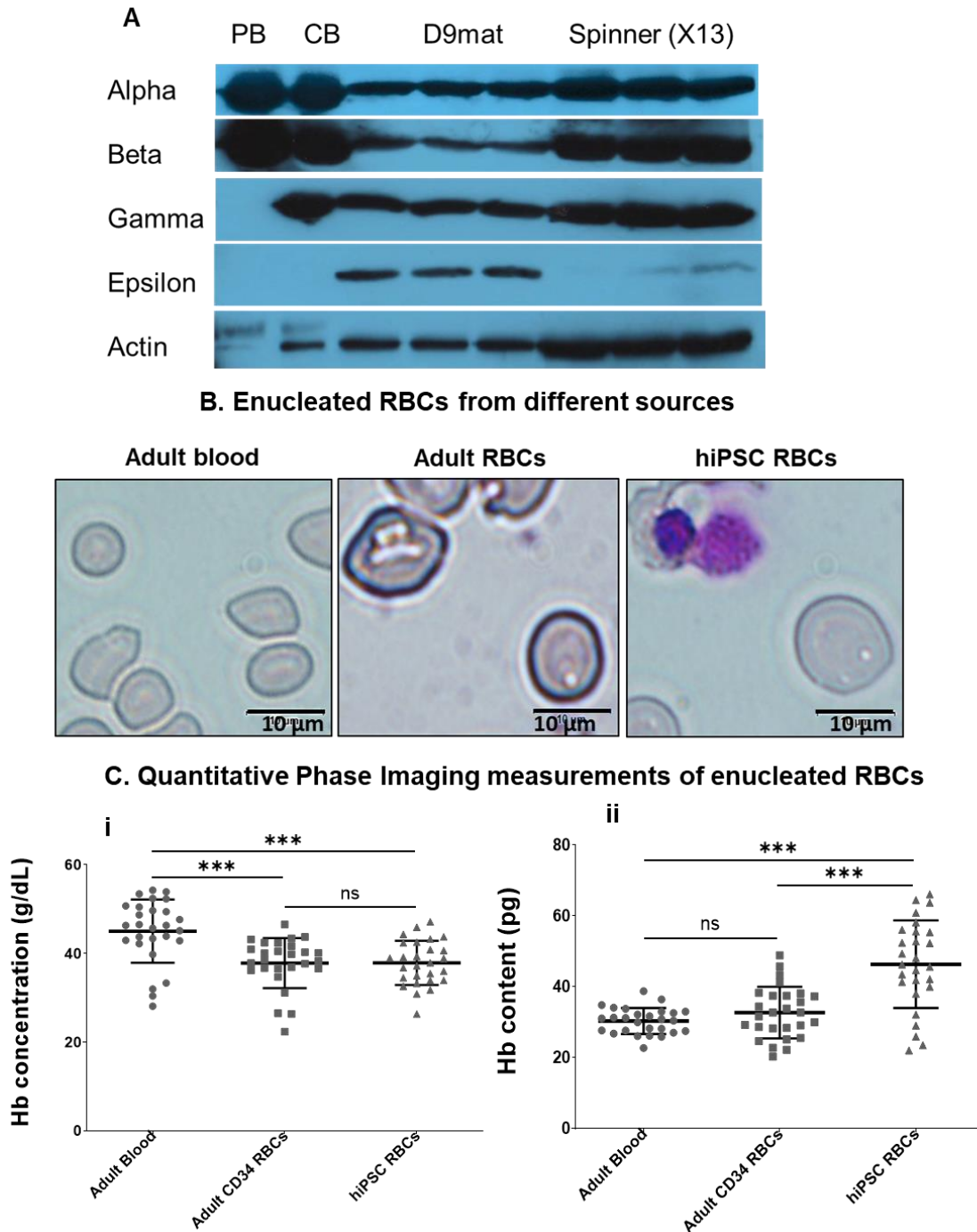
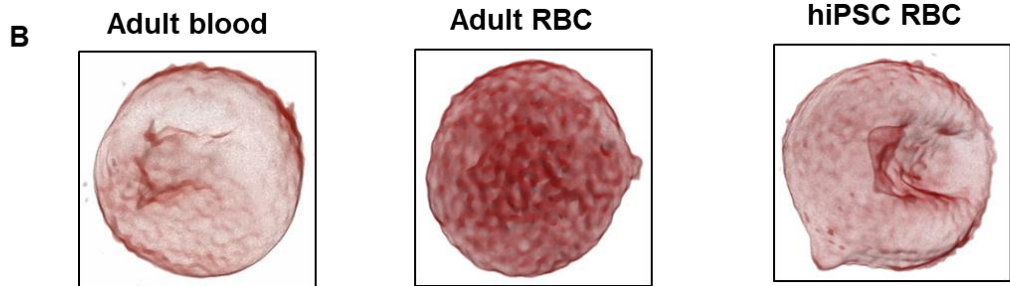
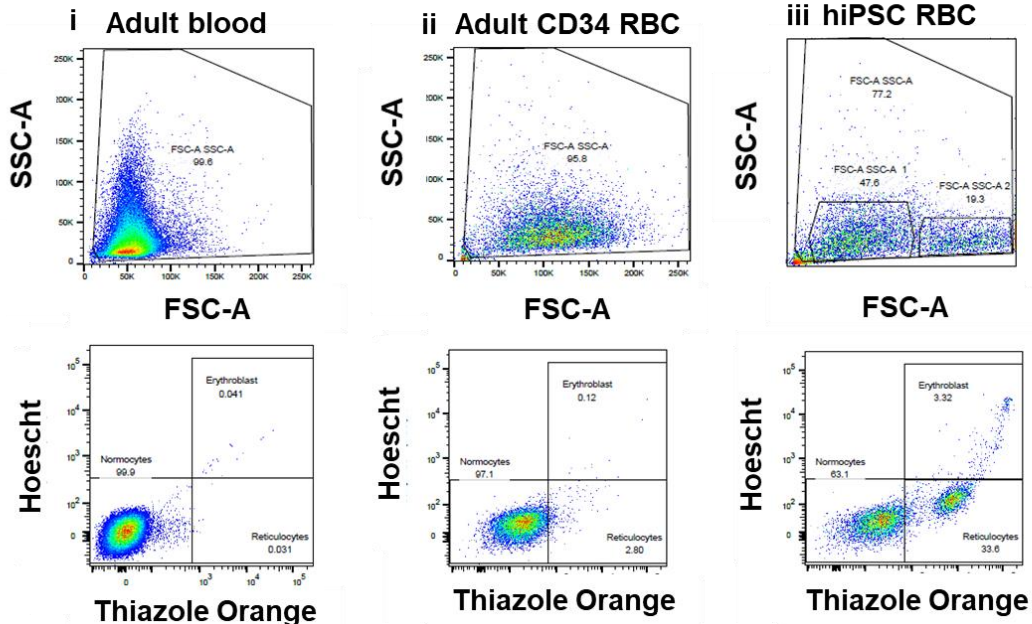


Figure S6: Terminal maturation and functional characterization of hiPSC and adult CD34 differentiated RBCs. (A) Entire western blot with expression of globin subtypes that shown in Figure 5A (CB and D9 mat are not involved in this study). (B) Giemsa staining of enucleated RBCs from adult blood, Adult differentiated RBCs and hiPSC differentiated RBCs. Scale=10 micron. (C) Quantitative phase imaging data for (i) Hb concentration and (ii) Hb content measurements for RBCs from the 3 different populations using a HT-2S Holotomographic microscope.

Figure S7 Terminal maturation and functional characterization of hiPSC erythroblast

A. Flow cytometry characterization of reticulocyte and normocyte populations



C. Electron microscopy imaging of enucleated RBCs

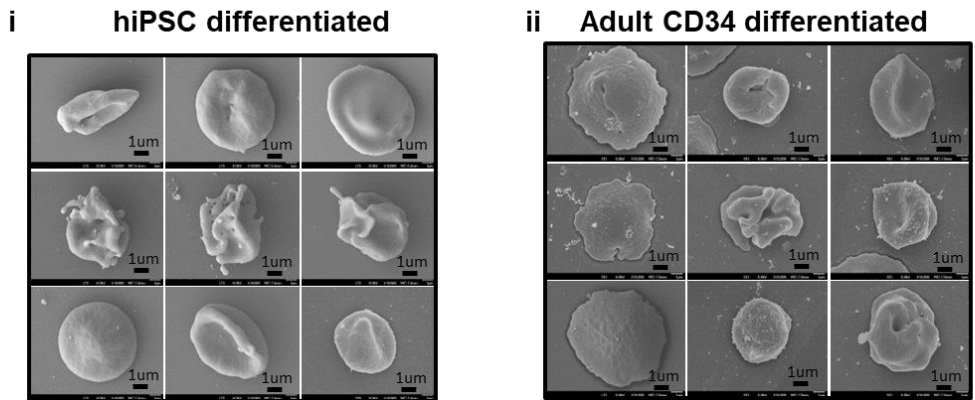


Figure S7: Terminal maturation and functional characterization of hiPSC and adult CD34 differentiated RBCs. (A) Flow cytometry characterization of purified RBCs from (i) adult blood and in vitro differentiation of (ii) adult CD34 and (iii) hiPSCs. Cells were stained with Hoechst and Thiazole Orange dyes to quantify percentage of normocytes, reticulocytes and erythroblast which are identified in their specific quadrants in the flow cytometry plots. (B) 3D-tomography representative images and (C) scanning electron microscopy images of enucleated RBCs from the respective groups. Scale=1 micron.

Supplemental Experimental Procedures

Monolayer pluripotent cell culture

O-neg hiPSC lines (D5, D9, D12, X13, BR7) were reprogrammed from CD71+ erythroblasts, derived from finger-prick blood of consented human donors (with approval from the ethics committee of the National University of Singapore; approval number NUS 1957) as detailed previously (Chen et al., 2016, Tan et al., 2014). FR202 was reprogrammed similarly using dermal fibroblasts. IMR90-iPSC was kindly provided by James Thompson's lab (Yu et al., 2007). BM1 (IISH1i-BM1) and CB6 (IISH3i-CB6) hiPSCs were purchased from WiCell Research Institute. All hiPSC lines were cultured as detailed previously (Sivalingam et al., 2016).

Microcarrier pluripotent cell culture

Culture of hiPSCs on MCs has previously been described (Sivalingam et al., 2018, Sivalingam et al., 2016). 3D MC-hiPSCs were cultured under continuous agitation in an agitated platform at 75 rpm for 7 days with daily medium changes. For initiation of spinner cultures, hiPSC-MCs initially cultured for 7 days under static condition in 6 well ULA plates were manually broken into small aggregates by gentle pipetting and seeded in 50 ml of mTeSRTM1 medium at a density of 2×10^5 cells/ml. Cells were cultured in 125 ml spinner flasks (Corning) at 36 rpm with 90% medium change daily for 7 days.

Hematopoietic mesoderm induction of hiPSC-MC aggregates

HPSC-MC aggregates (1×10^6 cells/ml) were transferred to mesoderm induction medium composed of cytokines plus Stemline ®II Hematopoietic Stem Cell Expansion medium (SL2) (Sigma-Aldrich) in either 6 well ULA plates (5 ml) under continuous agitation at 75 rpm or 125 ml spinner flasks (50 ml) under continuous agitation at 36 rpm. Daily medium changes as indicated: **Day 0**- SL2 supplemented with 30 ng/ml BMP4 (R&D systems), 50 ng/ml VEGF-165 (Peprotech), 40 ng/ml Activin A (StemcellTM Technologies), 15 μ M CHIR-99021 (Selleckchem); **Day 1**- SL2 supplemented with 30 ng/ml BMP4, 50 ng/ml VEGF-165, 40 ng/ml Activin A; **Day 2** - SL2 supplemented with 20 ng/ml BMP4, 30 ng/ml VEGF-165, 5 ng/ml Activin A, 10 ng/ml bFGF (Peprotech), 20 ng/ml SCF (R&D systems) and 0.4 ng/ml β -estradiol (Sigma-Aldrich). Samples were collected on day 1 and day 3 for flow cytometry analysis of T-brachyury (T-Bra) and KDR+ cells, respectively.

Hematopoietic induction of cells derived from hiPSC-MC aggregates

On day 3 of differentiation, single cells were derived from hiPSC-MC aggregates following treatment with TrypLETM Express (ThermoFisher Scientific) at 37°C for 5 min followed by straining through 40 μ m cell strainers (Greiner Bio-one, Germany). Cells were seeded at $1 - 2 \times 10^5$ cells/ml in hematopoietic induction medium (adapted from Olivier *et al* (Olivier et al., 2016)) in either 6 well ULA plates (5 ml), 50 ml shake-flasks (10 ml), 125 ml spinner flasks (50 ml) or 500 ml spinner flasks (100 ml). Complete medium changes (unless otherwise stated) as indicated: **Day 3**- SL2 supplemented with 20 ng/ml BMP4, 30 ng/ml VEGF-165, 10 ng/ml bFGF, 30 ng/ml SCF, 10 ng/ml IGF2 (StemcellTM Technologies), 10 ng/ml TPO (Peprotech), 5 U/ml Heparin (Sigma-Aldrich), 50 μ M 3-Isobutyl-1-methylxanthine (IBMX)(Sigma-Aldrich), 0.4 ng/ml β -estradiol; **Day 5**- Top-up 1:6 with SL2 supplemented with 120 ng/ml BMP4, 180 ng/ml VEGF-165, 60 ng/ml bFGF, 180 ng/ml SCF, 60 ng/ml IGF2, 60 ng/ml TPO, 30 U Heparin, 300 μ M IBMX and 2.4 ng/ml β -estradiol; **Day 7** – SL2 supplemented with 20 ng/ml BMP4, 30 ng/ml VEGF, 10 ng/ml bFGF, 30 ng/ml SCF, 10 ng/ml IGF2, 10 ng/ml TPO, 5 U Heparin, 50 μ M IBMX, 0.4 ng/ml β -estradiol. **Day 9** - Top-up 1:2 with SL2 supplemented with 20 ng/ml BMP4, 30 ng/ml VEGF-165, 10 ng/ml bFGF, 30 ng/ml SCF, 10 ng/ml IGF2, 10 ng/ml TPO, 5 U Heparin, 50 μ M IBMX and 0.4 ng/ml β -estradiol.

Erythroid induction of cells derived from hiPSC-MC aggregates

Cells were seeded at $1 - 2.5 \times 10^5$ cells/ml in erythroid induction medium in either 6 well ULA plates (5 ml), 50 ml shake-flasks (10 ml) or 125 ml and 500 ml spinner flasks (50 -100 ml). Complete medium changes (unless otherwise stated) as indicated: **Day 11**- SL2 supplemented with 6.7 ng/ml BMP4, 30 ng/ml SCF, 50 μ M IBMX, 1 μ M hydrocortisone (Sigma-Aldrich), 16.7 ng/ml Flt3L (Peprotech), 6.7 ng/ml IL3 (Peprotech), 4 U/ml EPO (Peprotech); **Day 13**- Top-up 1:6 with SL2 supplemented with 40.2 ng/ml BMP4, 180 ng/ml SCF, 300 μ M IBMX, 6 μ M hydrocortisone (Sigma-Aldrich), 100.2 ng/ml Flt3L, 40.2 ng/ml IL3, 24 U/ml EPO, 3 μ M Pluripotin (Sigma-Aldrich); **Day 15 onwards** - SL2 supplemented with 1X serum replacement 3 (Sigma-Aldrich), 0.3% v/v ExCyte reagent (Millipore), 1 μ M hydrocortisone, 100 ng/ml SCF, 4 U/ml EPO, 10 ng/ml IL3, 0.2 mg/ml holotransferrin (MP Biomedicals) and 1X Penicillin and Streptomycin (Gibco). Cumulative fold-expansion was calculated by multiplying fold-expansion achieved between passaging of cells over the course of study.

Terminal maturation of erythroid cells

Terminal maturation of erythroid cells was induced by transferring cells to maturation medium ($1-2 \times 10^6$ cells/ml) for 14-21 days with medium change every 3 days; Iscove's Modified Dulbecco's medium (IMDM) (ThermoFisher Scientific) supplemented with 10% human plasma (Innovative™ Research), 10 ng/ml human recombinant insulin (Gibco), 6 U/ml EPO, 1 μ M mifepristone, 500 μ g/ml holo-transferrin and 1X Penicillin-Streptomycin. In some experiments, erythroid cells were co-cultured with bone-marrow derived primary human MSCs or murine OP9 stromal cell-lines (a gift from Dr. Wang Shu's lab at IBN, A*STAR) either seeded on tissue culture 6 well plates (1×10^5 cells/well) under static condition or on microcarriers (2×10^5 cells/20 mg of Solohill microcarriers) in 6 well ULA plates under continuous agitation at 70 rpm. Enucleated cells were enriched by passing through non-woven fabric filters (Tao et al., 2011)(Antoshin, Singapore) or Acrodisc WBC Syringe filters (Pall). Detection of enucleated cells was performed by flow cytometry analysis of live cells stained with 1:100 diluted CD235a-FITC, 1:100 diluted Annexin V and 1:5000 dilution of a cell-permeable nuclear dye, DRAQ-5™ (eBioscience).

RNA extraction and quantitative real-time PCR

Cell samples were lysed in Trizol® reagent (ThermoFisher Scientific) and stored at -80°C until time of RNA extraction. RNA-extraction with DNase-treatment was performed using Direct-zol™ RNA extraction kit (Zymo Research). RNA samples were quantified by O.D260 nm measurements using a NanoDrop UV-Vis spectrophotometer (ThermoFisher Scientific).

500 ng of total RNA was used for 1st strand cDNA synthesis using iScript™ Advanced cDNA synthesis kit (BioRad). cDNA samples diluted 1:10 in RNase-free water were used for quantitative PCR using gene-specific primers (**Table S2**), iTAQ™ Universal SYBR® green supermix (BioRad) and Applied Biosystems® 7500 FAST Real-time PCR system (ThermoFisher Scientific). GAPDH was used as a house-keeping gene for normalization of sample quantities. Relative change in gene expression was determined using the delta-delta c(t) method(Livak et al., 2001).

Immunoblot

Protein extraction, immunoblotting and detection of immunocomplexes were performed as previously detailed (Sivalingam et al., 2018) with the following primary antibodies [1:800 diluted beta-globin (Santa Cruz, SC-21757), 1:400 diluted gamma-globin (Santa Cruz, SC-21756), 1:2000 diluted alpha-globin (Santa Cruz, SC-31110), 1:400 diluted epsilon-globin (Abcam, ab156041) and 1:2000 diluted Actin (Santa Cruz, SC-1615) and relevant secondary antibodies (horse-radish peroxidase (HRP)-conjugated anti-mouse IgG (Jackson ImmunoResearch), HRP-conjugated anti-rabbit IgG (Jackson ImmunoResearch), or HRP-conjugated anti-goat IgG (Jackson ImmunoResearch) at dilution of 1:10000).

Microarray study

Erythroid cells were differentiated from X13-hiPSC according to the method described earlier. Hematopoietic cells from adult peripheral blood from X13 donor were differentiated into erythroid cells by culturing in erythroblast expansion medium for 2 weeks. RNA was extracted from 1 to 2×10^6 cells per sample using Direct-zol RNA MiniPrep Kit (Zymo Research, Irvine, CA). RNA integrity was evaluated using Agilent 2100 Bioanalyzer (Agilent Technologies, Santa Clara, CA) and samples with RNA Integrity Number ≥ 8 were used for expression analysis. Labelled single-stranded cDNA targets were prepared from 250 ng total RNA using the GeneChip WT PLUS Reagent Kit (Life Technologies, Carlsbad, CA) and assayed on the Human Clariom D Array according to manufacturer's protocol. CEL files were extracted from Affymetrix GeneChip Command Console (AGCC) and quality assessment of the CEL files was carried out using Transcriptome Analysis Console (TAC). Raw data from CEL files was RMA-normalized and summarized to transcript clusters using R 'oligo' package. The expression level of genes consisting of multiple transcript clusters was based on the transcript cluster with the highest average expression across samples. Genes with expression value ≥ 6.68 in at least three samples were deemed to be expressed. This threshold was derived from the 95th percentile of background control transcript clusters. Differential gene expression analysis was carried out using Limma. Genes with absolute fold-change ≥ 1.5 and FDR-adjusted p -value < 0.05 (Benjamini-Hochberg method) were deemed as differentially expressed. Volcano plots for comparison between the different groups showing $-\log_{10}$ FDR-adjusted p -value in the y-axis and average \log_2 fold-change in the x-axis were plotted using R. Heat maps of average linkage clustering of gene expression between samples were derived using Heatmapper with Euclidean used for measuring distance between rows and columns (<http://heatmapper.ca/expression/>) (Babicki et al., 2016). Venn diagrams for comparison of DEGs between different groups were done using on-line available tool from VIB-UGent Bioinformatics and Evolutionary Genomics Group (<http://bioinformatics.psb.ugent.be/webtools/Venn/>). Gene ontology of biological processes for DEGs was derived using PANTHER classification system (<http://www.pantherdb.org/>). Gene list for selected categories were derived from Kyoto Encyclopedia of Genes and Genomes (KEGG; <https://www.genome.jp/kegg/>), Gene Ontology resource (<http://geneontology.org/>), Human

MitoCarta 2.0 (<https://www.broadinstitute.org/files/shared/metabolism/mitocarta/human.mitocarta2.0.html>) and Lux et al (Lux et al., 2016). Fold-change in expression of selected DEGs (adult vs hiPSC erythroid cells) specifying important molecular functions was verified by RT-qPCR and compared with microarray data.

Flow cytometry (FACS)

Flow cytometry was performed as previously detailed (Sivalingam et al., 2018) on cells fixed with 4% paraformaldehyde (eBioscience) using NovoCyte Flow cytometer (ACEA Biosciences Inc., USA) and analysed using FlowJo Software. The following antibodies were used for measuring: pluripotency [primary antibodies: 1:100 Oct4 (R&D Systems, USA); 1:50 Tra1-60 (Millipore), 1:100 SSEA4 (BioLegend, USA) and secondary antibody: 1:500 diluted rabbit anti-mouse IgG-FITC conjugate (DAKO)], mesoderm [T-brachyury-FITC (R&D Systems), KDR-PE (Miltenyi Biotec), CD31-PE], hematopoietic marker [CD34-APC, CD43-FITC, CD 45-PE, CD71-APC, CD235a-FITC, CD14-APC, CD15-APC, CXCR4-APC, CD133-FITC (all from BD Biosciences, USA)]. The following antibodies were used as isotype-controls: mouse IgG1-FITC and PE (Miltenyi Biotec, Germany), mouse IgG2b_k-FITC and mouse IgG2a_k-APC (BD Biosciences). For hemoglobin analysis, 0.1% v/v Triton X-100 permeabilized cells were incubated with 1:50 diluted fetal hemoglobin-FITC (ThermoFisher Scientific) or adult hemoglobin-PE antibodies (Santa Cruz Biotechnology, USA). Annexin V staining was performed according to manufacturer's instruction using 1:100 FITC Annexin V antibody (Biolegend). Quantification of fresh normocytes, reticulocytes and erythroblasts were performed by co-staining with Hoescht and Thiazole orange using LSRII Flow Cytometer (BD Biosciences, USA).

Immunohistochemistry and microscope imaging

Cells were cytospun onto glass microscope slides (Marienfeld) using Cytospin™ 4 cytocentrifuge (ThermoFisher Scientific), fixed and stained using Giemsa stain (Sigma-Aldrich) as detailed previously (Sivalingam et al., 2018). Slides were imaged using Axiovert 200M inverted microscope (Zeiss). Immunofluorescence imaging of terminally matured erythroblast was done using Nikon Eclipse Ti-E fluorescence microscope (Nikon). All other cell images were taken using EVOS® Cell imaging system (ThermoFisher Scientific).

Oxygen equilibration curve

Hemox analyzer model B equipment (TCS Scientific Corp) was used to generate the oxygen binding and dissociation equilibration curves of cells as detailed previously (Sivalingam et al., 2018). Adult peripheral blood (donor derived) was run as controls. All samples were measured in duplicates.

Scanning electron microscopy

Electron microscopy was conducted on erythrocytes using the methods outlined in (Malleret et al., 2013).

Quantitative Phase Imaging using Holotomographic Microscopy

HT-2S Tomocube Holotomographic microscope (EINST Technology Pte Ltd) was used to perform 3-D quantitative phase imaging and optical diffraction tomography of single cells. The 3D refractive index (RI) distributions of the erythrocytes were obtained and morphological (cellular volume, surface area, sphericity), biochemical (hemoglobin concentration and content) and mechanical properties (dynamic membrane fluctuation) of RBCs were quantified from the reconstructed 3D RI tomograms using TomoStudio™ software. To obtain properties of the cells, voxels with higher RI than the background were selected. These segmented voxels provided the cell boundary and allowed for calculation of surface area (SA). Number of voxels also corresponded to volume of the entire cell, with cell volume (CV) = No. of voxels of the mask * unit volume. Sphericity was obtained directly from both CV and SA with the equation: Sphericity = $\pi^{1/3} * (6 CV)^{2/3}/SA$.

Cellular Hb concentration (CHC) was calculated based on mean refractive index (RI) of the cell – RI of the medium/ α , where α is a refraction increment of Hb and has a value of 0.2mL/g (Friebel et al., 2006, Park et al., 2009). Cellular Hb (CH) levels were then calculated with CH = CV*CHC*0.01.

The cell membrane fluctuations were obtained by first generating the 2D membrane fluctuation map which is defined as the temporal standard deviation of mean cell height profiles for the RBCs. The spatial average of this 2D membrane fluctuation map over the projected cell area provided the measure of membrane fluctuation (Lee et al., 2017, Park et al., 2016).

Statistical analysis

Statistical analysis was performed using GraphPad Prism 6 (GraphPad Software Inc.). Student's unpaired *t*-test was used for comparison between two groups with equal variance and the Mann-Whitney test was used when variances were not assumed to be equal. One-way ANOVA was used for multiple groups (more than 2 groups) comparison. Statistical tests were performed on the pooled data from at least 3 independent replicates. *P* values < 0.05 were considered significant. **p* < 0.05, ***p* < 0.01, ****p* < 0.001.